SAND2015-2042C

ILASS Americas 27th Annual Conference on Liquid Atomization and Spray Systems, Raleigh, NC, May 2015

A Modeling Method for Impact and Impulse Dispersed Liquids: Alternative Transfer Criteria and Sensitivity Analysis

A. L. Brown*, and F. Pierce
Sandia National Laboratories
Albuquerque, NM 87185-1135 USA

Abstract

A method has been previously described for predicting impact and impulse dispersion of contained liquids that employs SPH solid mechanics predictions to initialize Lagrangian/Eulerian fluid mechanics simulations. The coupling algorithm is based on a dimensionless length scale that defines the temporal exchange between the two codes. Previous work has identified grounds for formulating additional criteria to the coupling algorithm that will help create a more continuous transfer of mass and energy between the codes when performing these analyses. A new criterion is proposed based on a critical dimensionless energy formulated from a model for the surface and kinetic energy of binary pair systems of SPH particles. A model for the break-up of drops upon surface impact has recently been implemented in the SIERRA fluid mechanics code used for this work. The importance of this model to the quantitative results of relevant scenarios is not known, and is also explored herein.

Five scenarios simulated in the past exhibiting a variety of conditions provide the context for a sensitivity analysis that is used to quantify the importance of the new algorithms. The new dimensionless energy transfer criterion and the impact break-up model are of varying significance depending on the scenario. The effect of the impact break-up model is most significant for scenarios where the prediction of aerosol sized particles is important. The predictions are not particularly sensitive to the critical dimensionless energy parameter, however the dimensionless energy model exhibits a modest effect on the coupling. Data are needed to quantitatively validate these methods.

*Corresponding author: albrown@sandia.gov

Introduction

Liquid dispersal can occur due to the impact or impulse dispersal of contained materials. Such events can occur in transportation when fast moving vehicles are involved in collisions or exposed to detonations. They can also occur in industrial scenarios that involve reacting materials or elevated pressures. The subsequent environment is important because damage can be enhanced if the liquid is a fuel and becomes a component of a fire. Liquid dispersal can also be important when considering hazardous liquids. The physics of the initiating event is primarily structural/mechanical, whereas the ensuing environment is dominated by thermal/fluids physics.

After the events of September 11, 2001 there was a desire to predict the fire in the World Trade Center buildings that were primarily due to the impact of the aircraft into the structures. Simulations of the fire were not initialized directly with the results from the structural calculations [1].

Another effort has been made to predict this class of problems in the context of nuclear safety. They used experimental measurements of the liquid dispersion from a water impact test to initialize a spray [2].

Work by the authors and others at Sandia National Labs has focused on coupling the results from structural mechanics predictions to a fluid mechanics code [3-7]. The effort has shown to produce reasonably good predictive accuracy insofar as results have been compared with data. Five scenarios have thus far been considered. The scenarios capture a range of conditions, including different domain scale and variable liquid dispersal.

In this paper, we propose and explain the motivation behind the addition of a criterion to the coupling methodology for coupling a structural mechanics code to a fire code. The five scenarios used for past work will be revisited in the context of a comparison between the new and old methods. A drop shatter model was recently implemented in our fluid dynamics code, the addition of which is expected to be significant to certain scenarios. The results using the two new methods are compared back to the predictions without the models to quantify the importance of the new models to output metrics of interest.

Methods

The main point of a previous paper on this methodology was the need for a modification to the transfer criterion used in prior work [8]. It examined five previously simulated scenarios and showed that the dimensionless length scale criterion was not selecting certain components of the mass for insertion when it may reasonably be selected. The paper [8] is not expected to be easily accessible to readers of this work, so the results are briefly summarized herein. Five specific cases were selected from the suite of scenario runs for five physical scenarios. These are listed in Table 1. The scenarios involve a range of varied conditions including impact and impulse dispersal of the liquid, various fluid types, and a variety of length scales.

This work couples structural mechanics predictions with fluid mechanics predictions through a one-way coupling involving the smoothed particle hydrodynamics (SPH) modeling of a liquid in a finite element code to a finite volume computational fluid dynamics (CFD) code with a Lagrangian/Eulerian representation for drops. The temporal coupling is achieved through a dimensionless criterion, the dimensionless separation distance between the SPH particles. A dimensionless separation distance can be calculated for each SPH particle. When the minimum separation distance exceeds a critical value, the SPH particle is marked for insertion in the fluid mechanics code. The dimensionless separation distance is calculated as follows:

$$B_i = \min_{j=1\ to\ N} \left\{ \frac{\sqrt{(x_i - x_j)^2 + (y_i - y_j)^2 + (z_i - z_j)^2}}{{}^{d_i}/_2 + {}^{d_j}/_2} \right\}; i \neq j \tag{1}$$

In this equation, x, y, and z are the drop Cartesian coordinates, and N is the total number of homogeneous SPH particles. B_i is the minimum dimensionless separation distance for particle i. B_i is compared to B_{crit}, a user specified criterion normally between 1.0 and 1.7.

Table 1. Cases evaluated in this study

Scenario	Case	B_{crit}	SPH#	Reference
Water Slug Impact	Case 7	1.5	417,792	Brown et al., 2012 [5]
Aluminum Tank Impact	cfs1.3	1.3	19,653	Brown, 2010 [7]
Sled Track Brake	S1/F1	1.3	322,016	Brown and Metzinger, 2011 [6]
Detonation Outside Tank	Hex3 (Case 5)	1.3	49,152	Brown, 2013 [4]
Detonation Inside Tank	HighE	1.5	44,813	Brown et al., 2014 [3]

The solid mechanics predictions are often terminated based on the trends of the cumulative kinetic energy. This parameter normally stops changing significantly as time progresses, which is a good indication that the structural mechanics predictions are reaching the end of their valid regime. This does not guarantee that the liquid will be adequately dispersed by the final structural mechanical time step. There are often cases where some of the liquid remains in a bulk configuration. In this case, the mass usually is injected (even though it may not qualify as a dilute spray), and it often falls out of the fluid mechanics calculation quickly as gravity causes it to drop to a surface. Careful examination of the mass in the final injection suggested that there were instances where small groups of SPH particles were never selected for insertion by Equation 1. But the particle groups may represent primary drops that are larger than the SPH size. The potential for these groups can be estimated by counting the number of particles (n) within the $<B_{crit}$ range for each particle B_i.

The last file in each of the five cases was analyzed in this way to determine the relative frequency of particles that might fall into this category. Figure 1 shows the count for the five scenarios at the final injection. A gray dashed line highlights $n=2$. Below this level, there is a chance that the particle is in a binary system ($n=1$). There may be a system of three particles ($n=2$). For several of the cases, such particles represent a significant fraction of the total.

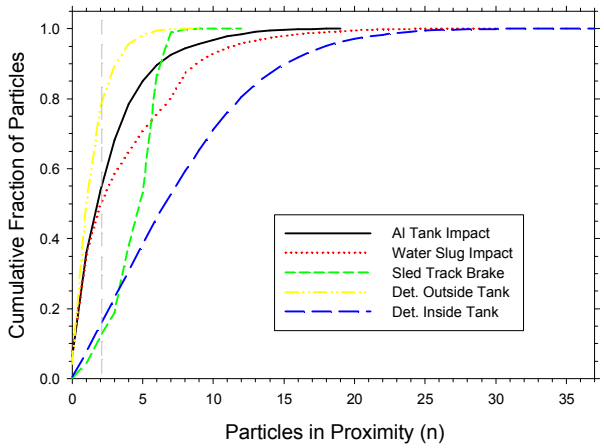

Figure 1. Cumulative fraction of particle systems that exhibit n particles within the B_{crit} threshold

Particles in Figure 1 with $n=1$ are candidate particles for combination. They may be simply a physical representation of a larger parcel of liquid than the fundamental SPH particle size. If the particle to which it is closest is also uniquely related to it (i.e., n=1 for both) and the mass is traveling in nearly the same direction and speed, the two may be combined. Figure 2 graphically illustrates the relationship with mass (m) and velocity (u) conditions along with a simplified abstraction of what that SPH condition may be representing physically. If the velocity differential between the particles is reasonably close, then the surface forces of the liquid will be able to overcome the separation force.

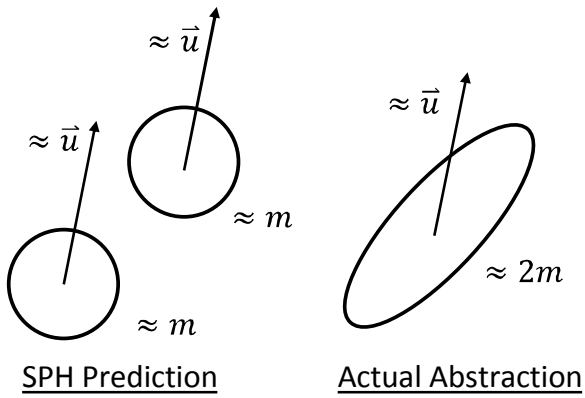

Figure 2. A simplified illustration of the potential interpretation of two SPH particles in close proximity with similar velocities.

For a quantitative way to assess the possibility of combining binary particle systems, a dimensionless energy criterion is used:

$$E_{dim} = SE/KE \tag{2}$$

Here E_{dim} is the dimensionless energy SE is the surface energy, and KE is the kinetic energy. A critical E_{dim} can be selected below which particles may be combined. This value should be near unity. The surface energy is modeled as that of the curved surface of a cylinder of mass $m_1 + m_2$ between the particle centers:

$$SE = \sigma A = \sigma h \pi D_e \tag{3}$$

where σ is the surface tension, A the area, h the cylinder height, and D_e the equivalent diameter, with the following definitions:

$$h = [(x_1 - x_2)^2 + (y_1 - y_2)^2 + (z_1 - z_2)^2]^{1/2} \tag{4}$$

where x, y, and z are the coordinates of particles 1 and 2, and:

$$D_e = 2\sqrt{(4/3)h(r_1^3 + r_2^3)} \tag{5}$$

where r is the radius of the particles. The kinetic energy is modeled as that of the difference between particles as such:

$$KE = (1/2)m\left|\vec{U}\right|^2 \tag{6}$$

Mass m is defined as the sum of the mass of the two particles:

$$m = \rho V = (4/3)\pi\rho(r_1^3 + r_2^3) \quad (7)$$

Here ρ is the liquid density and V is the particle volume. And velocity U is defined based on the difference in velocity between the two particles.

$$\left|\vec{U}\right| = [(u_1 - u_2)^2 + (v_1 - v_2)^2 + (w_1 - w_2)^2]^{1/2} \quad (8)$$

Here u, v, and w are the Cartesian velocity components for particle *1* and *2*. Particle pairs are combined by maintaining the kinetic energy and mass of the particle pair in a new single spherical particle centered at the mass centroid of the pair.

The selection of the surface area and the kinetic energy mass in the case of the present model might not be the best representation of these idealized quantities, but for the purposes of this model they will be shown in the results section to be adequate. Consider that they are not used as quantitative representations, rather in a dimensionless relation that involves the selection of a critical value. Preliminary work looked at the range of E_{dim} values that are common for particle pairs. A scatter plot of these data is found in Figure 3 illustrating the point. A gray dashed line indicates the model cut-off for E_{crit} of unity. Distributions are fairly uniform (i.e. not clumped). The kinetic energy varies significantly, whereas the surface energy only varies slightly from system to system. Thus, the precise value of the critical dimensionless energy was not thought to be a particularly sensitive parameter, and the details of the component models were thought to be equally insensitive. The velocity term appears to be the driving factor ($|U|^2$), and is well modeled. Model changes to the way mass and surface area are calculated will have a comparatively subtle effect. Results later in this report will further illustrate this point. The selected magnitude of E_{crit} can be varied moderately (moving the gray line left or right in Figure 3) with slight effect on the number of particles found to the left or the right of the line.

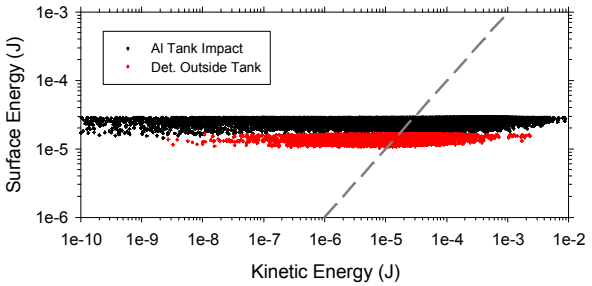

Figure 3. Surface energy versus kinetic energy for the final injection particle pairs for two cases.

Having developed a new method for defining the temporal coupling between a solid mechanics and fluid mechanics code, it is desirable to quantify the significance of this new paradigm to the predicted outcome of scenarios involving the coupled code predictions. The scenarios listed in Table 1 are used as a test bed for this effort.

The use of a critical E_{dim} for combining binary pairs is compared back to a base calculation, and quantities of interest from each simulation are extracted to see what effect the new model has on the outcome of the model prediction.

A drop shatter model has been developed in past work and was recently implemented in the fluid mechanics code base [9]. This model might also have a significant effect on the quantitative outcome of the predictions. The model is called a shatter model, but explained more accurately it uses dimensionless relations to predict one of three possible outcomes from a particle impact on a surface: 1. The drop impacts and shatters generating satellite drops; 2. The drop impacts and sticks to the surface; 3. The drop impacts and rebounds from the surface. A distinguishing component of this drop impact model is the model for predicting the uneven distribution of satellite drops in the event of a non-orthogonal impact.

As in most of the past work of this nature, the structural mechanics and fluid mechanics codes used are part of the SIERRA architecture. Past documentation can be examined for more details on the specifics of the predictive codes.

Results

The first comparison that is made is to demonstrate the sensitivity of the two critical dimensionless modeling parameters. The critical dimensionless length scale (B_{crit}) is varied from the baseline assumed in the source material (see Table 1) +/- 0.1. The critical dimensionless energy (E_{crit}) is varied by a factor of two increasing and decreasing. The cumulative dimensionless energy and cumulative dimensionless mass are plotted to illustrate the relative importance of these parameters to the temporal evolution of the coupling. The dimensionless mass, energy, and time are normalized such that the total reaches unity at the last time step. The normalization mass and time are constant for each case, but due to the time changing velocities in the structural mechanics code, the normalization kinetic energy changes depending on the selection of B_{crit} and E_{crit}.

Plotted in Figure 4 and 5 are the cumulative dimensionless kinetic energy and mass versus dimensionless time. The base case is labeled in the legends as the middle B_{crit} case and is plotted with a red solid line. Red lines (baseline original model cases) do not incorporate the dimensionless energy criterion, or may be

considered results for $E_{crit} = 0$ with the new theory. Blue lines all use the baseline B_{crit} value, but vary the value of E_{crit} as indicated in the legend.

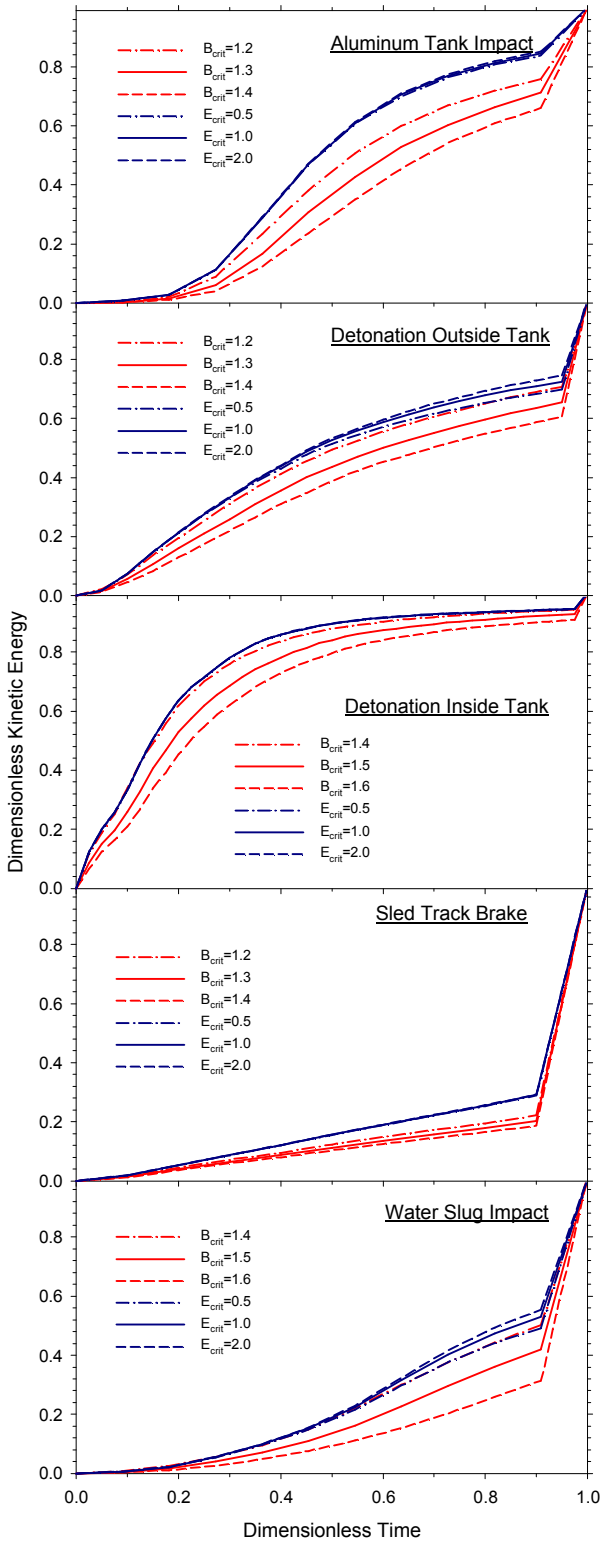

Figure 4. Cumulative dimensionless kinetic energy of injections for various B_{crit} and E_{crit} values.

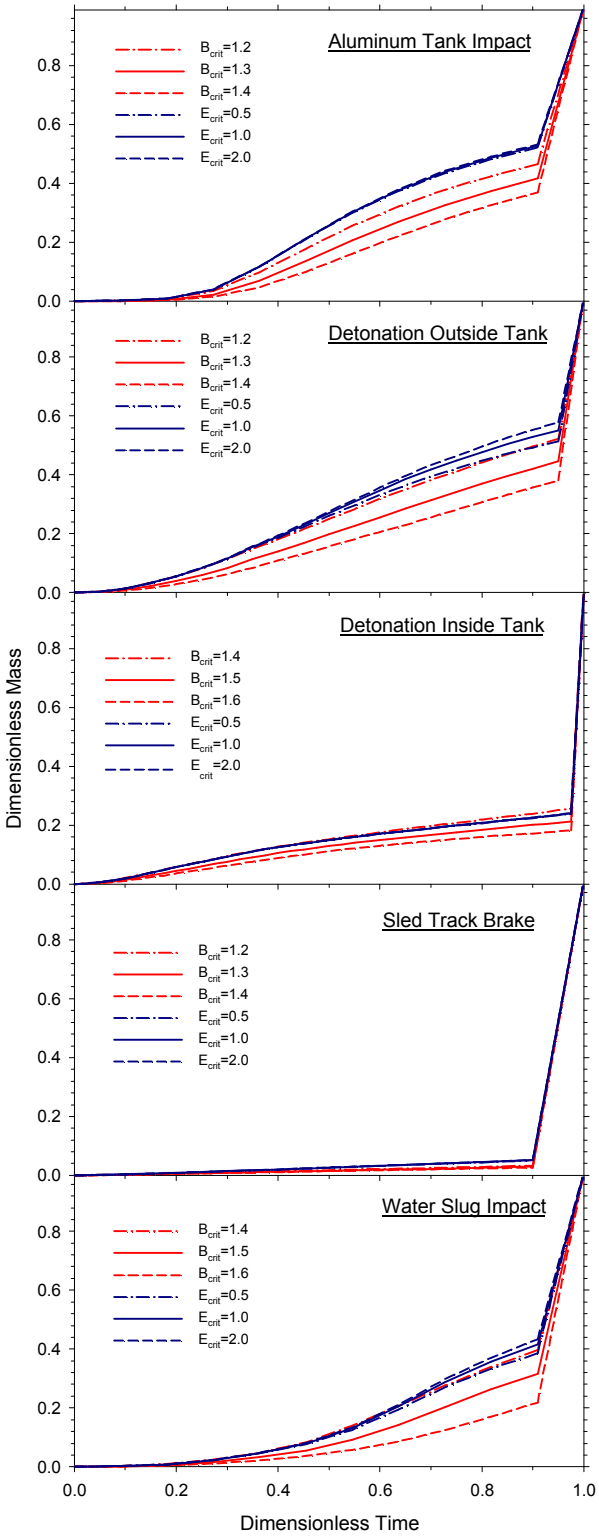

Figure 5. Cumulative dimensionless mass of injections for various B_{crit} and E_{crit} values.

These results show that the selection of B_{crit} is much more significant to the temporal coupling than the

precise selection of the E_{crit} parameter. Two of the cases (Water Slug Impact and Detonation Outside Tank) showed some sensitivity to the variations in E_{crit}, but the others scenarios were almost completely insensitive to a factor of two variation. The introduction of the E_{crit} parameter can be assessed by comparing the solid blue and solid red lines (baseline critical dimensionless parameters). The introduction of the baseline E_{crit} parameter results in changes equivalent to a change in B_{crit} of approximately 0.1 for most cases (sometimes more).

A challenge with this technology is that there are very limited data with which to quantitatively assess the accuracy of the models. In the absence of quality data, the model variations are assessed for quantitative significance by comparing predicted parameter results to step changes in model parameters. The parameters of interest for the scenarios outlined in Table 1 were not all the same. For the scenarios with hazardous fluids, the respirable mass fraction is important, and consequently the particle size distribution. The water and fuel spread problems might be more concerned with the distribution of the liquid on the ground or the size of the plume or fireball ensuing from the event. Evaporation relates significantly to the size of a fireball in a fuel dispersal problem, and that relates closely to the particle size parameters through the Sauter mean diameter (SMD), which is the average particle diameter best representative of the total surface area to volume ratio of the system.

The rest of the results section steps through the individual results from three calculations for each of the five scenarios. The 'Base' case uses the nominal value of B_{crit} for the scenarios with the exception of the Detonation Inside Tank scenario, which required a critical B_{crit} slightly higher for stability when used in conjunction with the E_{crit} parameter. The second scenario is the 'E_{crit}=1.0' scenario, and this case is the same as the base scenario except for the addition of the E_{crit} parameter. The final "shatter" scenario is identical to the base scenario except the shatter model is used. SMD versus time and a particle histogram at a selected time are shown in the body of the report. Corresponding visualizations of the results at a selected time are found at the end of the report.

Figure 6 shows the predicted SMD from the Detonation Outside Tank Scenario. Figure 7 shows the particle count binned to show the effect of the model on the distribution in the respirable range. Particle size is determined by the radius, the native size parameter in the code. The effect of the shatter model was pronounced, with significantly more particles predicted and a lower shift in the particle size distribution as indicated by a smaller SMD. At 1 second, the number of particles in the 5 μm range is nearly an order of magnitude higher for the shatter model scenario than for the base scenario. The effect of the dimensionless energy criterion is also evident. It is not as pronounced as the shatter model, but still enough to shift the SMD by a slight amount and shift upward the particle count at the low size range.

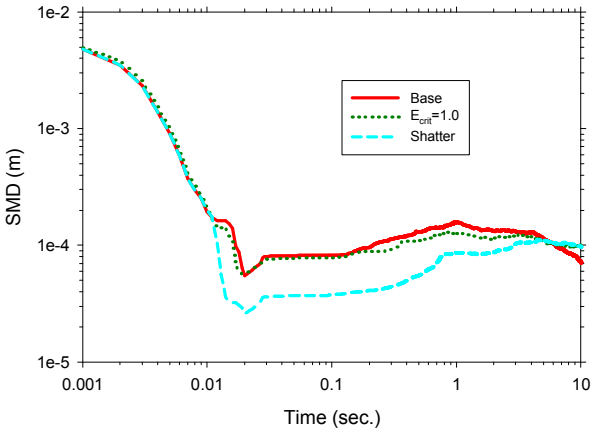

Figure 6. Sauter Mean Diameter predictions for the Detonation Outside Tank Scenario.

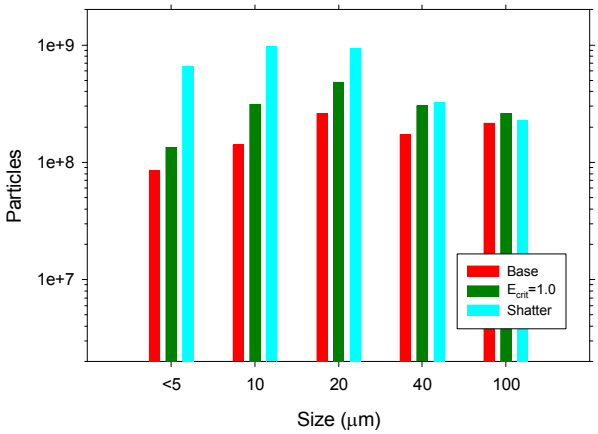

Figure 7. Particle histogram predictions for the Detonation Outside Tank Scenario at 1.0 seconds.

The similarly formatted results of the Detonation Inside Tank scenario are shown in Figures 8 and 9. Recall from earlier discussion that these results are for B_{crit} = 1.6. This particular scenario did not exhibit as much sensitivity to the variations. The SMD predictions for each parametric case were mostly similar, and the particle histogram shows a subtle effect of the parametric variations on the particle size distribution. A curious finding is that the dimensionless energy criterion exhibited the greatest number of particles. This is due to the fact that the mass from the last time step was not injected. This means that using the dimensionless energy criterion caused an increase in the mass in the system for this scenario. The other scenarios injected all the mass at the last time step, so this feature is not present in any of the other predictions. The shatter

model resulted in a small increase in the particle count in the two lowest bins compared to the base scenario.

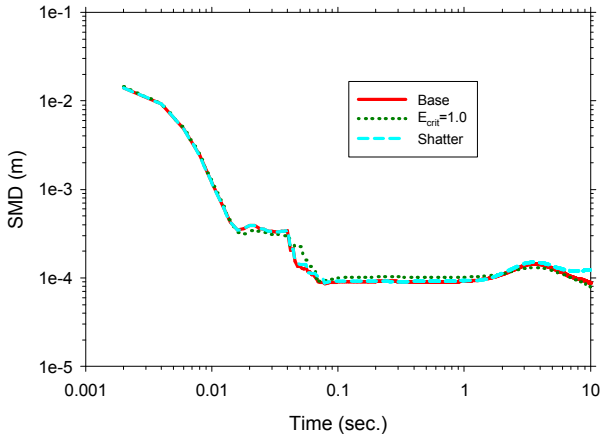

Figure 8. Sauter Mean Diameter predictions for the Detonation Inside Tank Scenario.

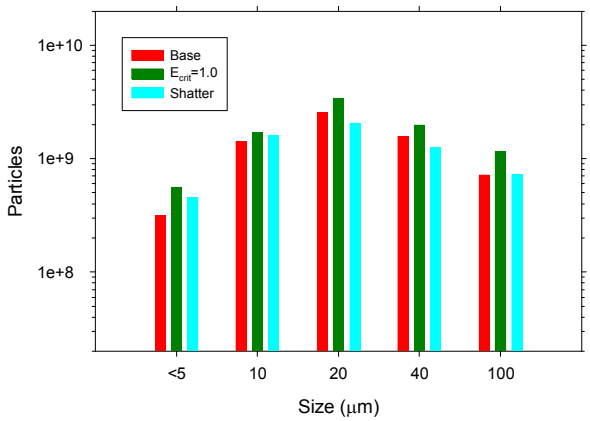

Figure 9. Particle histogram predictions for the Detonation Inside Tank Scenario at 5.0 seconds.

The next scenario evaluated is the Aluminum Tank Impact scenario. The shatter model was not expected to show significant effect because the fluid was a fuel, and the most of the fuel was actively burned in a fireball shortly after the initial impact. There was no significant ground deposition, and there were relatively few particle-surface impacts. The dimensionless energy criterion had the potential to be the more significant parameter for this scenario.

The SMD results for the Aluminum Tank Impact scenario are found in Figure 10. Around 0.004 seconds there is a significant difference between the baseline and shatter case and the dimensionless energy criterion case. This is a brief excursion from what is otherwise a very similar trend for all three cases. This is likely due to enhanced aerodynamic break-up of particles for the base and shatter cases during the injection phase of the calculation. There is some particle ground impact at the early times from the initial downward spreading mass, but this is lofted in a buoyant plume at around the impact time. Later on (2-5 seconds time), there are more ground impacts involving liquid that was spread laterally in the initial pulse which was not consumed in the fireball. Detailed particle size distributions were extracted at 2.5 second, and these results are plotted in Figure 11. The base scenario did not predict any drops existing below 20 μm at this time. The dimensionless energy criterion scenario predicted a few, while the shatter model had significantly more. This is consistent with the expected results based on SMD predictions in Figure 10. The SMD for the shatter scenario is slightly lower than for the other two cases after about 2 seconds. Note the comparatively low particle count for this scenario in the scale of Figure 11 presumed to be due to the consumption by the fireball.

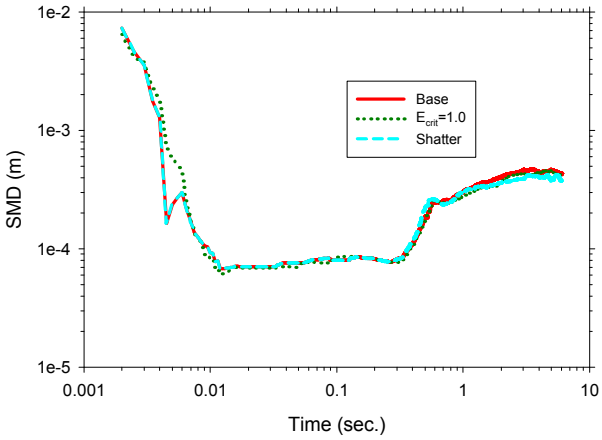

Figure 10. Sauter Mean Diameter predictions for the Aluminum Tank Impact Scenario.

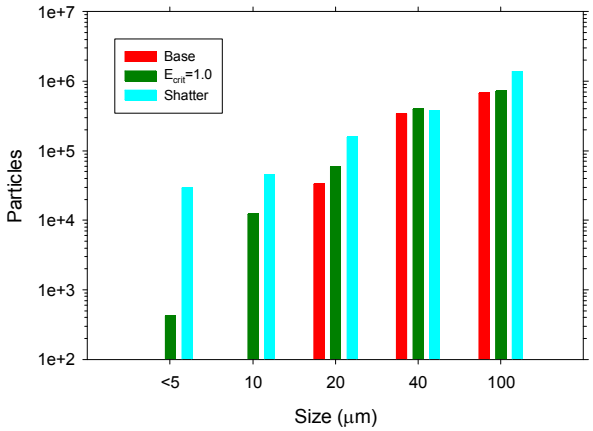

Figure 11. Particle histogram predictions for the Aluminum Tank Impact Scenario at 2.5 seconds.

The fourth case is the sled track scenario. The SMD results for this scenario shown in Figure 12 did not show much sensitivity to either of the parametric variations. Similarly, a histogram of the particles is

found in Figure 13 taken at 3.5 seconds. The parametric variations exhibit only slight changes in the extracted variables. This doesn't mean that the two parameters are not important. Consider Figures 4 and 5 that show that the majority of the mass is injected at the final time step. This final bulk injection appears to dominate this scenario. The visualization at the end of the paper for this scenario shows significant differences in the ground mass deposition as well as in the particle distribution. These do not show up in either Figure 12 or 13 because the bulk region tends to dominate the particle count and the distribution.

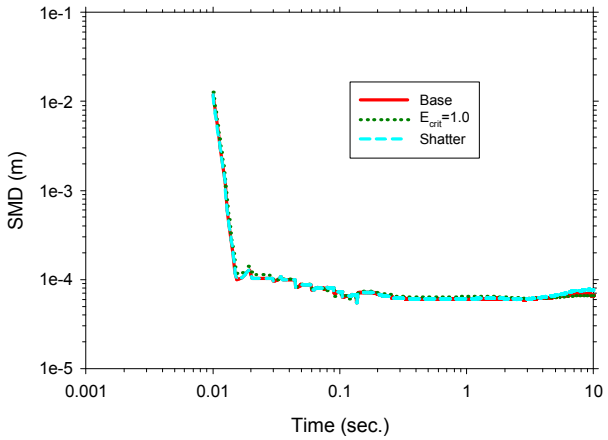

Figure 12. Sauter Mean Diameter predictions for the Sled Track Brake Scenario.

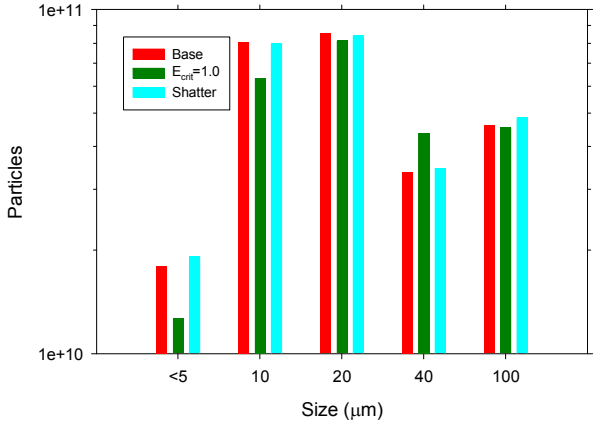

Figure 13. Particle histogram predictions for the Sled Track Brake Scenario at 3.5 seconds.

The last scenario is the Water Slug Impact scenario. The SMD is plotted in Figure 14, while the particle histogram predictions at 4.0 seconds are found in Figure 15. The shatter model and the dimensionless energy model both appear to result in a slightly lower SMD through the first second. The shatter and base cases converge to similar results thereafter, while the case with the dimensionless energy continues with lower SMD. The histogram suggests that the shatter model mostly results in increased particles in the higher size (20-100 μm) range compared to the base case, while the dimensionless energy scenario appears to result in the highest number of particles in the lower size range (20 μm and below).

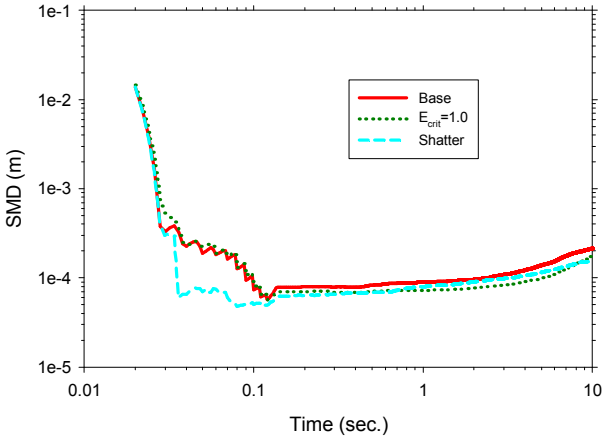

Figure 14. Sauter Mean Diameter predictions for the Water Slug Impact Scenario.

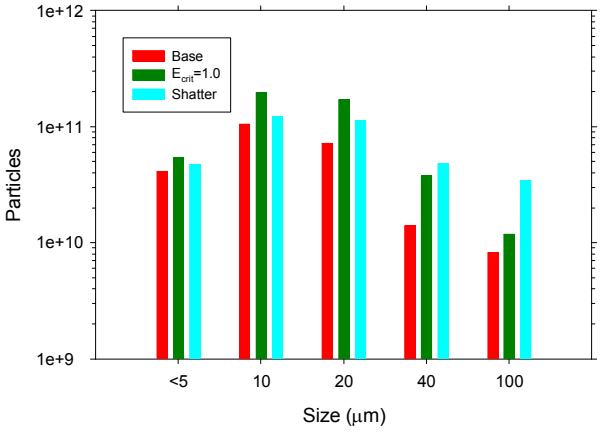

Figure 15. Particle histogram predictions for the Water Slug Impact Scenario at 4.0 seconds.

General Discussion

A surprising finding from these simulations is the relative lack of importance of the shatter model on the predicted size distribution and SMD of particles for several of the scenarios. Prior to the quantitative assessment, it was suspected that the shatter model would show a remarkable effect in some scenarios. It was, however, not particularly important in many of the quantitative plots. It usually resulted in an increase in the particle count at the lower size range, but the effect was often insignificant. The most significant effect on SMD was for the Detonation Outside Tank scenario, a case where most of the liquid rained onto the surface

after the impulse. Figures 16 through 20 at the end of this report suggest that the deposition patterns on the ground are significantly affected. This is normally expressed in a wider distribution or a more smooth distribution of mass after the test. This was most evident for the Detonation Inside Tank scenario, the Water Slug Impact scenario, and the Sled Track Brake scenario. This effect was not as apparent in the SMD or in the particle size histograms. This suggests that there is a more dominant physics occurring related to the particle size, which is thought to be the aerodynamic break-up model. As described in earlier work [3-8], the Taylor Analogy Break-up (TAB) model [10] is currently being used. This suggests that the TAB model is important, and often appears to be the determining factor in the particle sizes and size distributions.

The use of the dimensionless energy parameter is a useful addition to the modeling methods. Its use does not normally have a dominant effect on the prediction results, but seems to have a moderate effect on the particle size distributions. This is likely due to TAB model interactions as well, and has to do with the earlier advancement of particles into the fluid code. The methods section suggests that the selection of the surface area and mass parameters could be improved, but this is probably not warranted. The existence of a dimensionless energy parameter has a moderate effect. The model is generally insensitive to the quantitative magnitude of the critical dimensionless energy. This insensitivity suggests a similar insensitivity to the other two (SA and mass) parameters as well. This model will likely be used in subsequent work.

The purpose behind the dimensionless energy criterion was to capture a large number of particle pairs that were being ignored for transfer when using just the dimensionless length scale parameter for coupling. The fact that the use of the parameter had impact is suggestive of the importance of using it in the future. The last injections still contain a significant fraction of the energy and mass in many of the cases (see Figures 4, 5). There is an interest in having a better way to model this mass and energy in the future because the models are not expected to be particularly accurate in this regard. It is thought to be morphologically complex and not thought to consist uniquely of drops as is presently assumed. The structural mechanics code does not have the correct physics for modeling surface tension, which becomes increasingly important. The fluid code needs additional methods for treating multi-phase behavior of dense liquid to better model the behavior of the liquid core. This remains a topic of future research.

One reason the wall shatter model was not found to be particularly significant may have to do with the use of an evaporation model combined with very dry initial conditions. The small drops generally formed by surface impact had a finite lifetime because they were prone to evaporation. While this study found surprisingly low sensitivity, it may be found to be of increased sensitivity if one considers in the future a case where the liquid does not evaporate or the ambient environment is closer to the saturation point. This analysis is left to subsequent work.

It would be helpful to perform a sensitivity analysis in the context of a comparison to data. There are very limited data appropriate for assessing model predictions. It would greatly improve confidence in the prediction results if such data were available.

Conclusions

A dimensionless energy criterion is proposed for enhancing the ability to predict coupled structural mechanics and fluid mechanics liquid dispersion problems. The theory and motivation are presented, and the particle velocity is found to be the most significant quantitative parameter to the model outcome.

The new methods are compared to the old methods for five scenarios. The critical dimensionless energy criterion exhibits mass and energy shifts comparable to a shift in the dimensionless length-scale criterion of about 0.1. The dimensionless energy criterion has a minor effect on particle size distributions.

A sensitivity analysis including a shatter model was performed. Neither model variation was particularly significant to the particle size distributions and particle mean sizes (SMD). The shatter model exhibited a moderate effect on the surface deposition in several of the cases.

Acknowledgements

Sandia is a multiprogram laboratory operated by Sandia Corporation, a Lockheed Martin Company, for the United States Department of Energy under Contract No. DE-AC04-94AL85000.

References

1. Gann, R.G., Editor, "Final Report on the Collapse of the World Trade Center Towers, NIST NCSTAR 1, Washington, D.C. USA, September 2005.
2. Silde, A., Hostikka, S., and Kankkunen, A., *Nuclear Engineering and Design*, 241, pp. 617-624, (2011).
3. Brown, A.L., Feng, C., Gelbard, F., Louie, D., and Bixler, N.E., The 2014 ASME/AIAA Summer Conference, Atlanta, Georgia, June 16-20, 2014.
4. Brown, A.L., *The 2013 International Seminar on Fire and Explosion Hazards*, Providence, RI, USA, May 2013.

5. Brown, A.L., Wagner, G.J., and Metzinger, K.E., *Journal of Thermal Science and Engineering Applications*, 4:2:021004-1 to 021004-10, (2012).
6. Brown A.L., Metzinger, K.E., *The ASME/JSME 2011 8th Thermal Engineering Joint Conference*, AJTEC-44422, Honolulu, HI, USA, March 13-17, 2011
7. Brown A.L., *The 2010 Western States Meeting of the Combustion Institute,* Paper # 10S-12, Boulder, CO, USA, March 21-23, 2010.
8. Brown, A.L., *The 2014 JANNAF conference*, SAND2014-19543C Albuquerque, New Mexico, USA, December, 2014.
9. Brown A.L., Jepsen, R.A., *ASME 2009 IMECE Conference,* Lake Buena Vista, FL, USA, IMECE2009-11675, November 13-19, 2009.
10. O'rourke, P. J., and A.A. Amsden, "The TAB Method for Numerical Calculation of Spray Droplet Break-up," *SAE Technical Paper* 870289, 1987.

Additional Plots

The next five plots are frames corresponding to the particle size histograms presented in earlier work. These are component frames of videos that the authors will use during the oral presentation of this work.

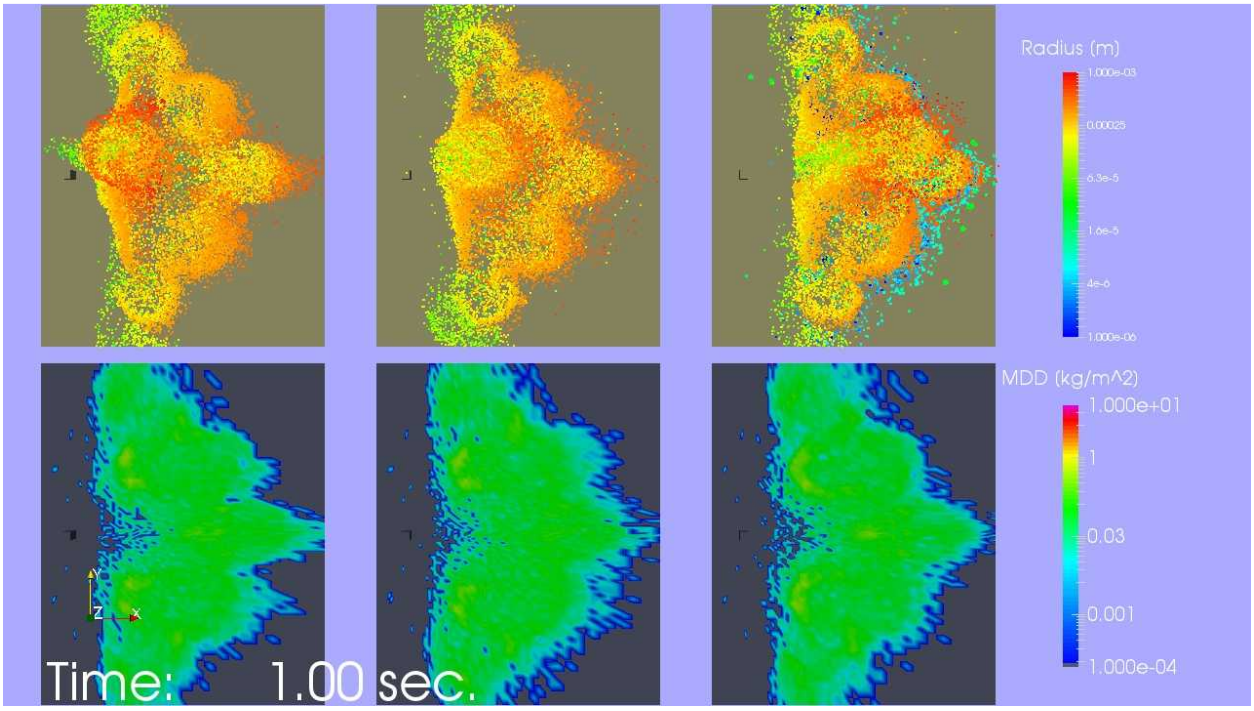

Figure 16. A contour plot of the ground mass deposition density (bottom) and the particle parcels (top) colored by radius for the Detonation Outside Tank scenario. The three scenarios are from left to right the base case, the E_{crit} = 1.0 case, and the shatter case.

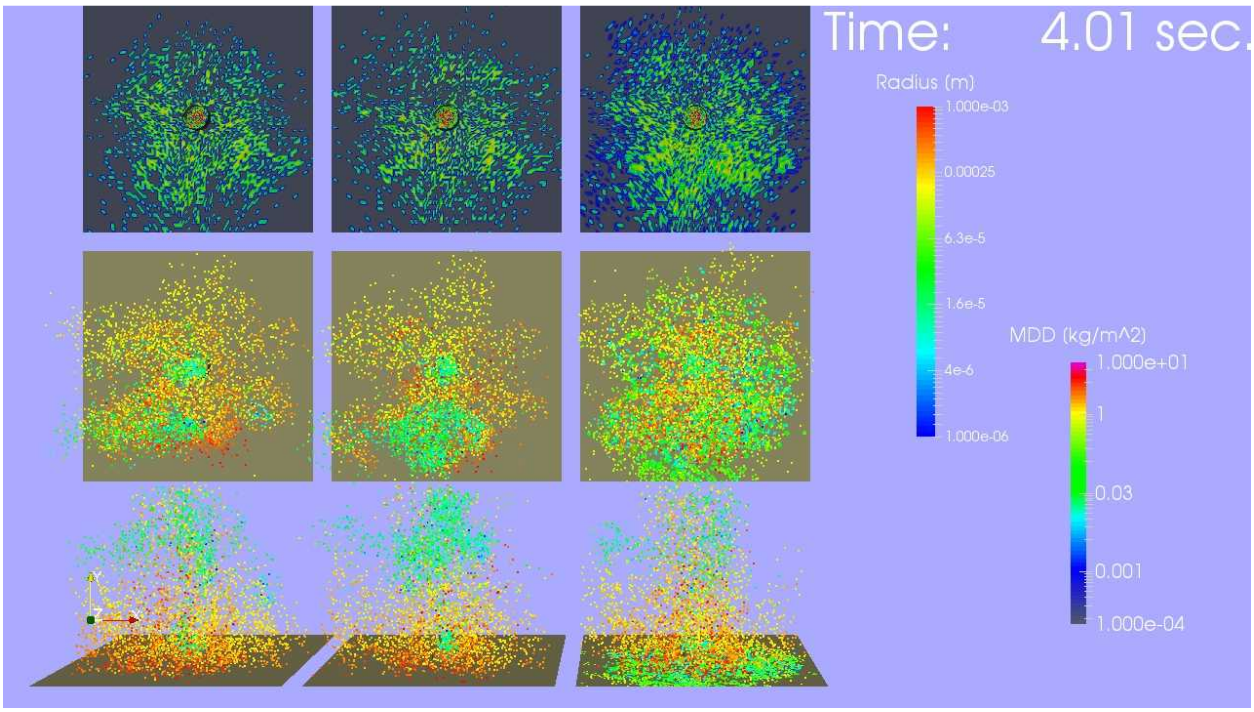

Figure 17. A contour plot of the ground mass deposition density (top) and the particle parcels (middle and bottom; top and side views) colored by radius for the Detonation Inside Tank scenario. The three scenarios are from left to right the base case, the E_{crit} = 1.0 case, and the shatter case.

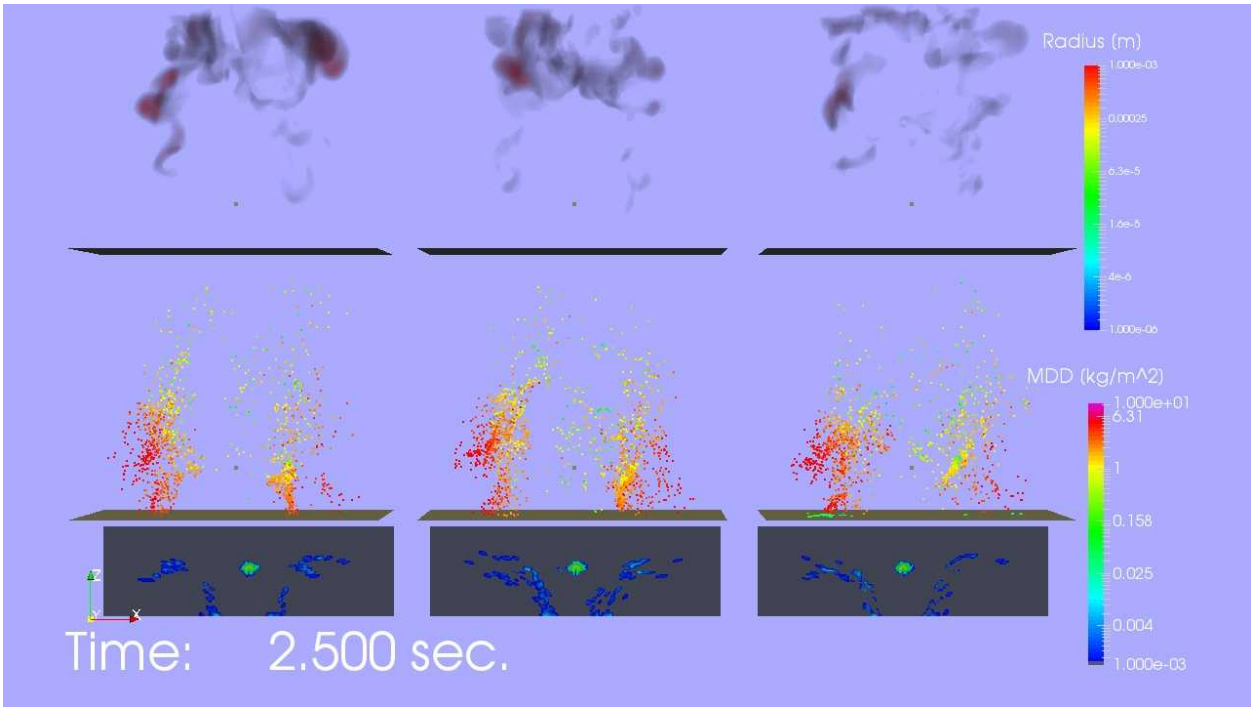

Figure 18. A contour plot of the ground mass deposition density (bottom) and the particle parcels (middle) colored by radius for the Aluminum Tank Impact scenario. The top frame is a volume rendering of the fireball based on the predicted temperature. The three scenarios are from left to right the base case, the E_{crit} = 1.0 case, and the shatter case.

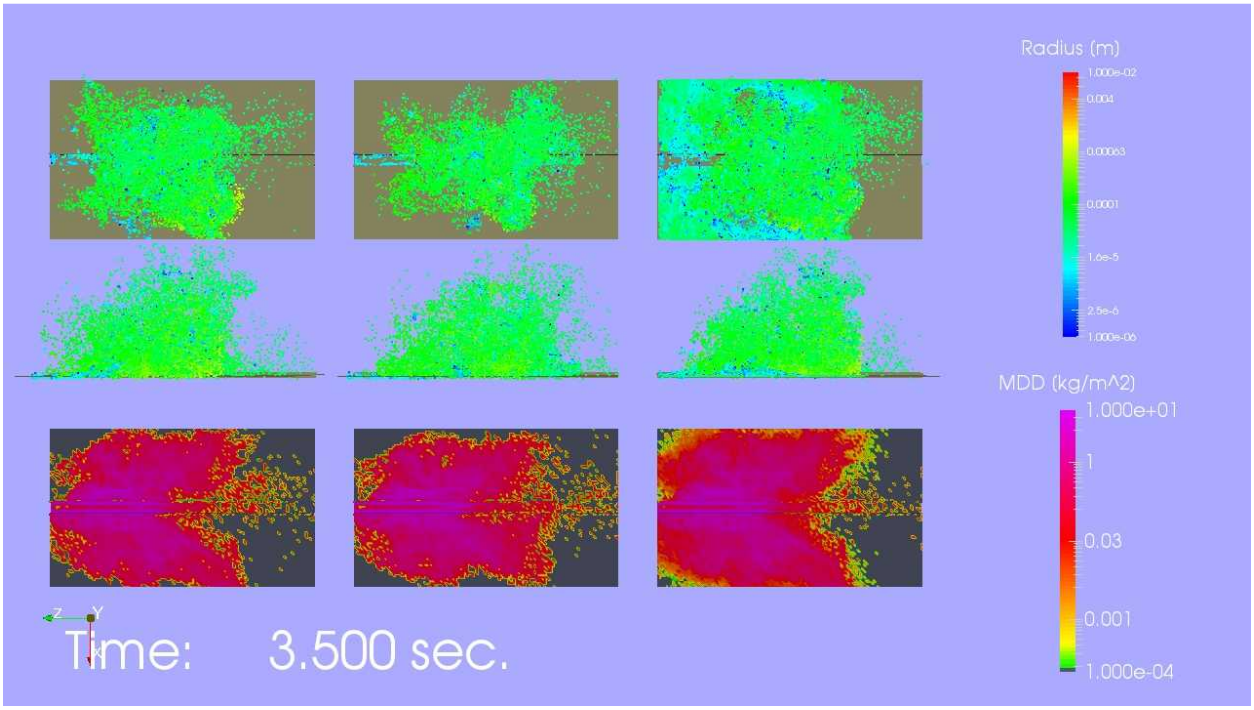

Figure 19. A contour plot of the ground mass deposition density (bottom) and the particle parcels (middle and top; side and top views) colored by radius for the Sled Track Brake scenario. The three scenarios are from left to right the base case, the E_{crit} = 1.0 case, and the shatter case.

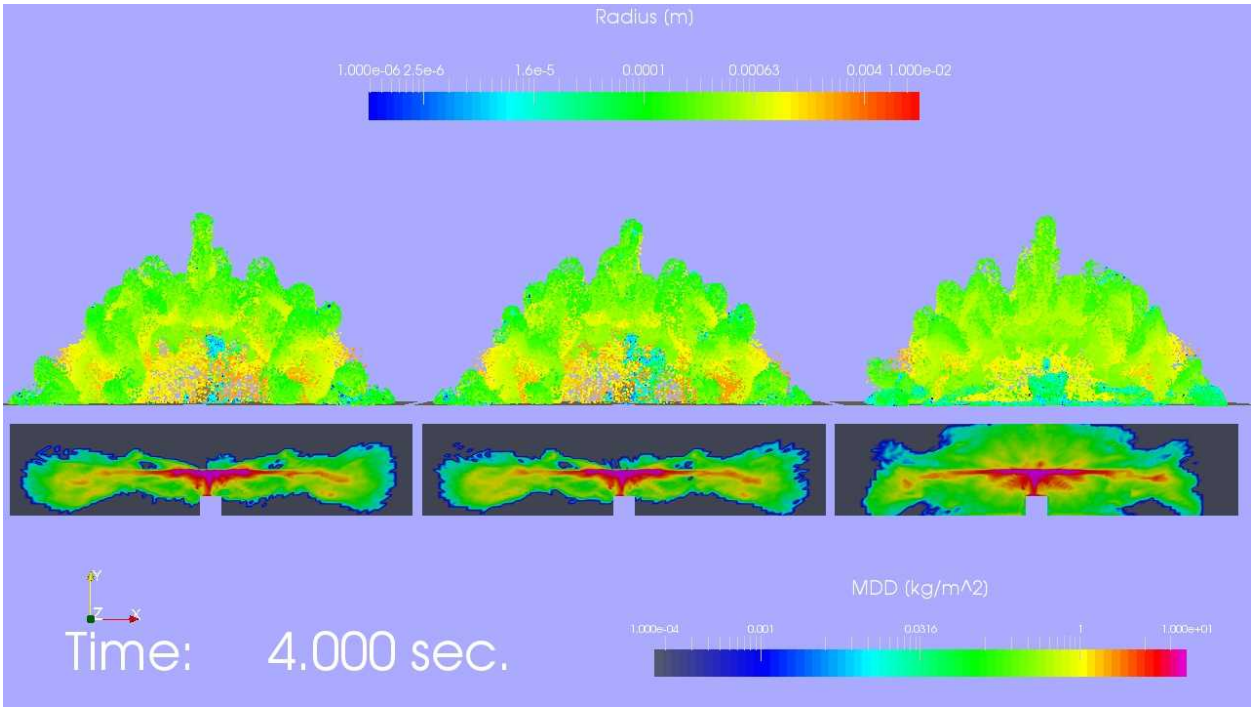

Figure 20. A contour plot of the ground mass deposition density (bottom) and the particle parcels (top) colored by radius for the Water Slug Impact scenario. The three scenarios are from left to right the base case, the E_{crit} = 1.0 case, and the shatter case.